The Thesis Committee for Alex Leviyev
certifies that this is the approved version of the following thesis:

Nanowire Sharpening:
Application to Field Ionization

APPROVED BY

SUPERVISING COMMITTEE:

_____

Mark Raizen, Supervisor

_____

Richard Fitzpatrick

Nanowire Sharpening:

Application to Field Ionization

by

Alex Leviyev, Bachelor of Science, Physics

Thesis

Presented to the Faculty of the Graduate School of

The University of Texas at Austin

in Partial Fulfillment

of the Requirements

for the Degree of

Master of Arts

The University of Texas at Austin

January 2019

Dedicated to my amazingly supportive family, and my new nephew Anthony, without whose support this would not be possible.

Acknowledgments

I'm extremely grateful to have been given the opportunity to work with the Raizen Group. In particular, I'd like to thank Mark Raizen from the bottom of my heart for inviting me, and instilling in me a desire to look for ambitious problems to work on. The last few years have been formative. Being in the trenches has not only provided me with context and hard skills, but has also given me perspective on the types of problems I enjoy working on.

Thanks to all the amazing people in the Raizen group that took an active role in mentoring me as well. Particularly Georgios, Yu, Kevin, Pavel, and Ahmed, who were always available to answer my questions with their sage-like patience. You guys are amazing, and I can only hope to help others the way you've helped me.

Special thanks to Jamie Gardner, the coolest physicist I've ever met, and his pastry baking prowess. Your cranberry muffins will never be forgotten...

ALEX LEVIYEV

The University of Texas at Austin
January 2019

v

Abstract

Nanowire Sharpening:
Application to Field Ionization

Alex Leviyev, M.A.

The University of Texas at Austin, 2019

Supervisor: Mark Raizen

Nanowires show potential for a wide range of fields, from developing next generation solar cells, to detecting viruses, to field ionizing gasses. Their uses in such disparate fields are due to the extreme flexibility in which nanowires can be manufactured and customized to order. The heart of a nanowire, however, is it's tip. Here surface charges accumulates in extreme densities when the wire is biased, consequently producing large electric fields that are then used in creative ways for exciting applications.

My aim for this thesis is three-fold. First, I intend to establish a context for nanowires. Why were these structures studied in the first place? What are some exciting application areas? What makes nanowires unique? Etc... This will set

the stage for subsequent sections, and provide the salt and pepper that will make the main course more flavorful. The second is to present an overview of relevant results from the literature that I will later build upon. There are analytical models of varying complexity examining the type of protrusions we are interested in here, as well as numerous numerical studies. We will look at them to get a deeper intuition for whats happening, and use them as a basis for comparison later on. Finally, I will present my results and discuss their consequences.

As we will see, sharpening a cylindrical-post nanowire of height $H = 1um$, starting radius of curvature $r_0 = 100nm$, and base size $b = 2 \cdot r_0 = 200nm$ can enhance the field further by an order of 100. In addition, the dielectrophoretic (DEP) force present due to strong electric field gradients can significantly alter cooled gas beam trajectories *towards* the nanowire tips. Non-cooled gas beams also display room temperature trajectory deviations for species with large polarizability to mass ratios. This leads to the conclusion that at lower temperatures (and even at room temperature) the field ionization cross section of a nanowire array is significantly increased under certain conditions when taking into account DEP coupling.

Table of Contents

List of Tables

List of Figures

Chapter 1

Introduction

1.1   A brief history of nanowires
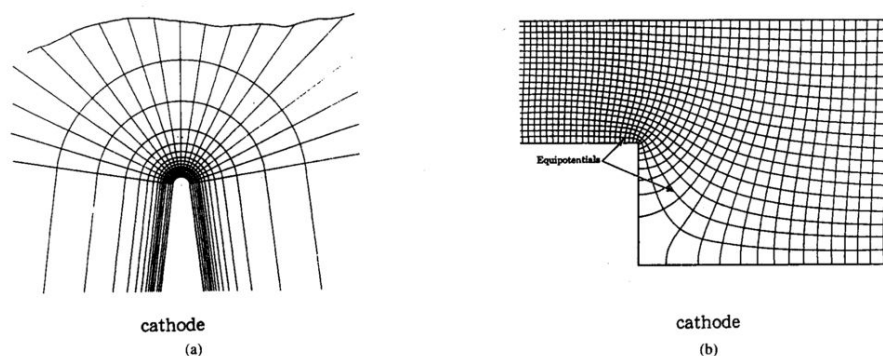
Figure 1.1: Two different schools of geometries. (a) Point-to-plain geometry. (b) Plane-to-plane geometry. Figure from [1]

.

Point-to-plain, post with taper, pointed protrusion, rounded whisker, conical post, etc... The protrusions that are the main topic of this thesis go by many names in the literature, but the idea is the same. Rigerously, these refer to a perturbation in shape of an otherwise flat electrode. In practice however, we are interested in the types of shapes that are analogous to pencils (if they were conducting). These pencil-like structures were originally looked at in the 1930's as a tool to confirm Fowler-Nordheim theory (abbreviated F-N) [1], which is a theory of cold field emission

of electrons from metals [5]. To obtain measurable current to test F-N theory, however, large electric fields are necessary. These electric fields could be produced by geometric enhancements, and that is where protrusions came to play: it was known that surface charges would accumulate near the tips of the wires producing great electric fields. The other option to consider if creating large electric fields is the goal are "plane-to-plane" geometries, which are simply sharp corners created by the geometric union of two planes.

It turned out that plane-to-plane geometries were plagued with dielectric breakdown problems. This was due to the impossibility of creating truly flat electrodes that are required in the plane-to-plane case. Interestingly enough, this would bring conical structures to the forefront in more ways than one. In the 1960's it was discovered that seemingly polished metal surfaces had "whisker like protrusions", which ultimately led to breakdown events. At the end of the day, the physics of arbitrary sharp extended protrusions (nanowire geometry falls under this category) were necessary to not only test F-N theory, but to explain dielectric breakdown mechanisms between flat electrodes. These original experiments are what spawned the study of possible applications: the first most clearly involving electron emission such as in vacuum microelectronics.

1.2   Applications

There are numerous application areas of this technology available for review in the literature. These are broken down into two categories: the first are semiconducting nanowires, and the most prevalent alternative are carbon nanotubes (which obey the same effects due to geometry as semiconducting nanowires, but differ in material physics). A few applications I find exciting will be referenced here for the interested reader.

Biological Sensing   For example, with proper doping a nanowire could be turned into a field-effect-transistor (FET), which has the property that the device's conductance is a function of a biasing voltage. If this is the case, changes in conductance due to this voltage could be measured and fingerprinted. This principle was exploited to test a sensitive and general purpose instrument that can detect biological and chemical specimen. In [6], researchers topped a nanowire with monoclonal antibody,

allowing them to to measure discrete changes in conductance when an influenza A particle binded to it. This opens up avenues for single virus detection, and can practically mitigate issues related to biological terrorism. In the medical field, this sensor could continue to impact disease diagnosis, genetic screening, drug discovery, and be used as an overall research tool in biology. This is important for biophysics research as well, considering time-series data and measurable potential differences would be invaluable for constructing theories of these processes.

Nanophotonics   Semi-conducting wires have found use in nano-photonics as well. For example, due to a nanowire's tight optical confinement and modularity, these structures have been shown to have practical applications as lasers, high-efficiency light emitting diodes, and single photon sources [7]. Recently, truncated nanowires have even been shown to have wide-band absorption properties. This means that these structures can utilize large proportions of incoming radiation from a source (such as the sun), and opens up possibilities for use as next generation solar cells [8].

Field Ionization: Gas Detection   The application of focus in this thesis, however, is the field ionization of gasses. Since extended protrusions enhance bulk fields, it offers possibilities to create sufficient enhancement for numerous applications while keeping operating voltages low (on the order of 100 V). For example, the breakdown characteristics of a particular gas can be used as a signature for detection applications [9]. An apparatus like this would have utility in numerous areas, such as in environmental monitoring and sensing in chemical plants.

Calcium-47 For Bone-Tumor Diagnosis   Yet another practical application could be the creation of a mass spectrometer. If a gas beam could be effectively ionized as it is fed into a nanowire array, then one could divert a beam uniquely depending on its charge to mass ratio. This could, for example, be used to create cost effective medical grade Calcium-47 for bone-tumor detection [10].

Nanowire arrays have the potential to provide a platform for scalable, low-voltage, high efficiency field ionization, with applications ranging from basic science to medical diagnosis. With this in mind, lets continue and talk about why nanowires have such pervasive utility.

3

1.3 What Makes Nanowires Different?

By controlling the growth process of the nanowires and their arrangement, various phenomena may be exploited for application in diverse areas from electronics to nanoscale photonic devices. Then, what gives nanowires such diverse utility? The answer is in the control of key parameters of the nanowire, and various bells and whistles that can extend functionality. For example, it is known that methods exist for controlling chemical composition, doping, structure, size, and morphology [11]. For example, axial and radial heterostructures can be constructed. What this means is a nanowire can be constructed, and different parts of the nanowire could be made of different constituents. For example, the base, the center, and the tip could all be made of different elements, or the p/n doped variants of the same element. This introduces extreme flexibility and variation in terms of introducing interesting material physics to utilize. This is exactly how the FET's discussed in Section 1.2 were created. Antibodies could be added to the tips to bind with viruses, or gold could be dabbed to introduce field enhancement via band-bending [12]. The well studied and numerous methods for constructed these wires, in addition a high degree of reproducability, allows these nanowires to have wide ranging utility.

Chapter 2

Theoretical Background

2.1 Nanowire Field Enhancement Studies
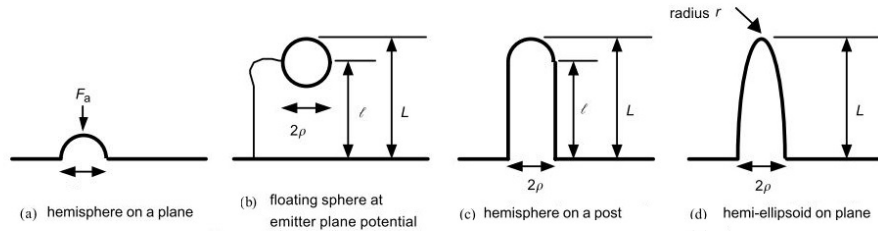
Figure 2.1: Various protrusion geometries. Figure from [2].
.

Protrusion geometries have been studied for quite some time, first coming into the spotlight to explain breakdown mechanisms between flat electrodes. Semi-conducting nanowires were then followed up with and studied for their application as field emittors, while the general theory of geometric enhancement was applied to other materials such as carbon nano-tubes. As a result, there exists a ladder of analytical models used to understand their behavior. To motivate the study of a sharpened nanowire, we will climb this ladder and summarize the main intuitions and results we'll need to make way for the following sections. We will begin with a hemisphere on a plane model, then proceed to a floating sphere above an electrode

geometry. We'll then follow up with the cylindrical nanowire geometry, move on to the more realistic hemi-ellipsoidal wire, and discuss a few related numerical studies.

2.1.1 Spherical Bump

We begin with a spherical bump geometry. Interestingly enough, this is the simplest model of a protrusion that exhibits field enhancement effects. Very simply, the geometry is comprised of a half sphere bump on a plane electrode (Figure 2.1a). This model has been studied and an exact analytical expression for the field enhancement factor (FEF) can be derived using the method of images. The field enhancement is given by $\gamma = \frac{E_{apex}}{E_{bulk}}$, where E_{apex} is the electric field at the apex of the geometric protrusion, and E_{bulk} is the electric field in the absense of that protrusion. Quoting the result, we have $\gamma = 3$ [2]. From here on, I will use as γ as a symbol to represent a protrusions FEF. There is one more step before we can look at a cylindrical post geometry. That being said, lets move on to the floating sphere next.

2.1.2 Floating Sphere

Next we look at a sphere that is biased at the same potential as a plane electrode (Figure 2.1b). It's not exactly trivial to see why this can be used to get useful results about a nanowire, however, that will soon become apparent. This model has the benefit that it can be addressed in a similar way to that of a spherical bump. A closed form exact solution can be derived with the use of bispherical coordinates, but instead we can use a series of approximations and obtain a result that is similar to the spherical protrusion geometry looked at in the previous section. The approximate FEF has the form $\gamma = 2.5 + \frac{H}{r_0}$, where H is the displacement of the center of the sphere from the biased plane, and r_0 is the radius of that sphere. Note that (Figure 2.1b) uses different notation to refer to the displacement and the radius, l and ρ respectively, however they are describing the same geometric properties. As we will see in the next section, the cylindrical wire geometry FEF can be expressed in a form very similar to this.

2.1.3 Cylindrical Wire

This is where things in the literature become interesting. A "unifying" expression is stated as $\gamma = 2 + \frac{H}{r_0}$, where unifying means of the same form as the previous

6

examples. Here r_0 refers to the radius of the hemi-spherical cap on top of the cylindrical wire. Note how two things are consistent through all the geometries we have looked at: a characteristic curvature which provides the enhanced field, and a "height" that separates the geometric regions of curvature with those that are flat. Note that if we set $H = r_0$, the result reduces to $\gamma = 3$, the correct limiting case for a spherical bump.

If we define the aspect ratio $\nu = \frac{H}{r_0}$, then we see that in the limit $\nu \to \infty$, $\gamma = \nu$. This is a rule of thumb expression that states that for $\nu \gg 3$ we can approximate the field enhancement as the aspect ratio. It was shown in [2], however, that this expression significantly over-predicts the field enhancement effects for large aspect ratios. A more accurate representation is

$$\gamma_{cyl} \approx .7\nu \tag{2.1}$$

within the range $30 \leq \nu \leq 2000$. A numerical study was conducted, and an extrapolating function of the form $\gamma = 1.2(2.15 + \nu)^{0.90}$ was developed to be valid to an accuracy of $\pm 3\%$ within the range $30 \leq \nu \leq 2000$. In general, the form of this numerical extrapolation is standard in the literature, and other authors cite the same form for similar but slightly different geometries as well. In other words, it is assumed that all protrusion FEF's are functions only of the aspect ratio ν by the following form:

$$\gamma = b(\nu + h)^c \tag{2.2}$$

where b, h, and c in this context are fitting parameters.

We will make sure that in Section 4.5, where the results of sharpening a cylindrical post are presented, that the results will asymptotically be in approximate agreement with Equation 2.1. I'll also present evidence supporting that $\gamma \approx \gamma(\nu)$ with no other functional parameters in Section 4.1.

2.1.4 Hemi-Ellipsoid

A general protrusion obviously will never be a perfect cylindrical post (unless specially designed to be so). We know that there will be a general curvature associated with the edges. Amazingly, a closed form and simple analytical solution exists that offers intuition on more realistic structures. If a quarter ellipse is drawn, and then

7

this figure is rotated around its major axis 360°, then this will produce an hemi-ellipsoid wire. It is not exactly the geometry that will be studied in this thesis, however, it provides an exact solution that could be studied analytically, and will be used in what follows to set upper and lower bounds on how a tapered cone geometry should behave. The result quoted as the analytical solution to a ellipsoidal protrusion is

$$\gamma_{ellipse} = \frac{\xi^3}{\nu ln(\nu + \xi) - \xi} \tag{2.3}$$

where ν is the aspect ratio of the wire, and $\xi = \xi(\nu) = (\nu^2 - 1)^{1/2}$.

2.1.5 Conical-Taper Analytical Bound
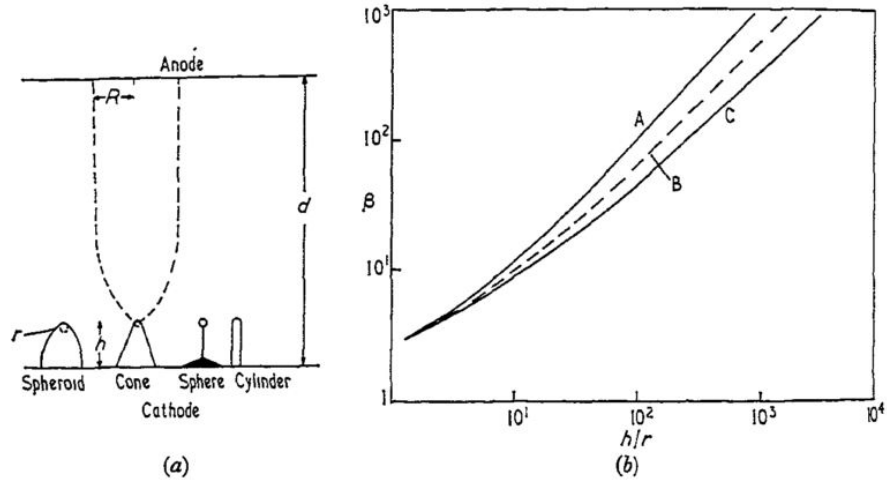
Figure 2.2: The basic geometry and variation of β with protrusion dimension is shown. (a) Basic geometry. (b) Variation of protrusion dimension: curve A, sphere or cylinder, curve B, cone; curve C, spheroid. *β here is the FEF, and a spheroid is a synonym for hemi-ellipsoid.* Figure from [3]

An exact analytical expression for the field enhancement factor of a cylindrical wire has not yet been derived, let alone a truncated cone (which is a generalization). Besides numerical simulations, an analytical analysis of conical tapered nanowires exists in the form of a bound study [3]. The author studies two limiting cases (the cylindrical protrusion and the ellipsoid), for which the truncated cylinder

8

can be thought of as something in-between. As expected, the results are all fairly similar, with the cone and spheroid of identical aspect ratio having FEF's that are slightly less than that of a cylindrical geometry. This makes intuitive sense because these geometries have a larger surface area, thus allowing surface charges to spread farther away from the tip.

2.1.6 Conical-Taper on Ball

Finally, we take a look at the most related paper on the results I will present in this thesis. The authors of [13] run computational analyses of carbon-tips grown via carbon contamination on tungsten balls. Numerical simulations are presented for a conical tip, however, the biased electrode is of a spherical shape and not flat like I intend to study here. Thus, any deviations from the main results presented in this referenced paper and the simulation results of this thesis can be attributed to numerical error, and variance between spherical and flat electrodes. The extrapolation is presented as

$$\gamma \approx 2.1(\nu + .8)^{0.73}. \tag{2.4}$$

As we expect, the numerical approximation is of the form previously stated (Equation 2.2).

Chapter 3

Mathematical Formulation

In this chapter I describe the details of how I define a conical-taper nanowire, how I specify the domain, and present the formulation of various studies undertaken. This section will clarify exactly what problem is being solved, how it is being solved, and why it is being solved that way. COMSOL Multiphysics is used for all simulations.

3.1   Nanowire Geometry

This section will present how I defined the conical-taper nanowire. The main result is a constraint equation which includes the base size, the radius of curvature, and the height of the nanowire. This expression must be satisfied for the union of a sphere and cone to be smooth.

   The goal with the following definition of the nanowire is to create a parameterized expression which controls the sharpness of the nanowire, and one that could easily be programmed. In order to do this, several things need to be taken into account.

1. Continuity of geometry: we want to avoid cusps. This is because sharp boundaries must be handled with care. The goal is to create a smooth geometry that will avoid all issues associated with cusps.

2. Parameterized expression that controls the nanowire characteristics. To run a sharpening analysis on these nanowires will require looping over various wire geometries. Doing that manually would be extremely tedious and time
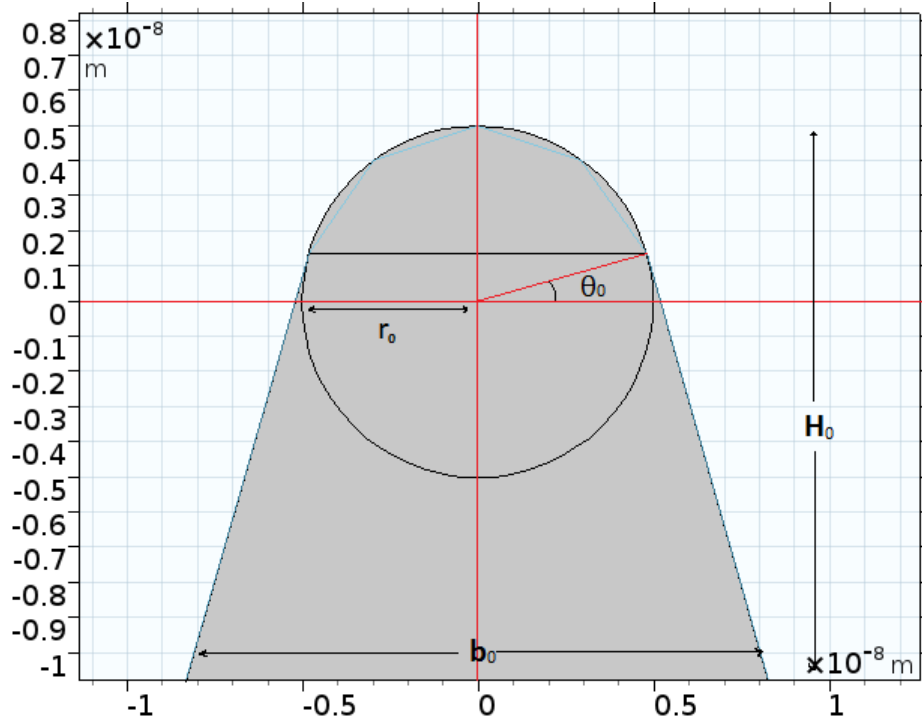
Figure 3.1: Cross section of nanowire geometry

consuming... Thus, a parameterized form of the nanowire would be ideal.

Smooth Sharpening   An ordinary nanowire (or nanopillar) can be thought of as a cylinder with a hemisphere glued to the top. A sharpened nanowire can still be thought of as a union between a section of a sphere and a cone, however, it is no longer a hemisphere that needs to be glued to the top, but a section of a sphere. As a result, there exists a constraint that must be met in order for the sphere and the conical sections to line up properly and form a smooth structure. This constraint can be derived and expressed as follows:

$$b_0 = \frac{2\left[r_0(1 - sin(\theta_0) - cot(\theta_0)cos(\theta_0)\right] - H_0}{-cot(\theta_0)} \tag{3.1}$$

where b_0 is the base of the wire, r_0 is the desired radius of curvature, and H_0 is the height of the wire. Here, θ_0 is a parameter which geometrically describes where the

11

stitching between the sphere and the cone must happen. Since b_0 is the physical parameter of interest here, finding the base size corresponding to a conical taper with a set H_0 and r_0 requires some numerical inversion scheme or guess and check procedure.

3.2   System Geometry

Our system is an ordinary parallel plate capacitor with several sharpened, conducting nanowires placed inside. This section is devoted to explaining how to convert this system into a working COMSOL simulation. Other formulations of this problem led to numerical instabilities, and overall failure for dependent variables to asymptotically approach known values in the literature. As we will see, smoothness, continuity, and a detailed study of the mesh is necessary to lead to accurate results.

Capacitor Geometry   The capacitor is a basic parallel plate capacitor. The mathematical formulation of this is two square surfaces a distance D apart. If we ignore boundary effects (ie, effects that happen near the edges of the nanowire array), then the only concern is that the domain is large enough to contain the nanowires, and allows the mesh to flow continuously between wires. To make this work, we define the size of the square plates as

$$S = 2H + 5b_0 + 4\delta \tag{3.2}$$

Where H is defined as the height of the nanowire, b_0 is the size of the nanowire's base, and δ is the pitch (center to center distance between nanowires). This means that as we increase the pitch between nanowires the solution domain increases by $O(\delta^2)$, making the computation time proportionally slower.

Array Geometry   In this simulation we model the array as a simple square lattice. Ignoring edge leads to a simple Braveis lattice, and this should be easily modeled by defining an appropriate unit cell with corresponding periodic boundary conditions. It is interesting to note, however, that this approach led to field solutions that were clearly not physical. To circumvent this issue, I decided to pick a nanowire in the middle of our "infinite" array, and see what effect the surrounding nanowires had on
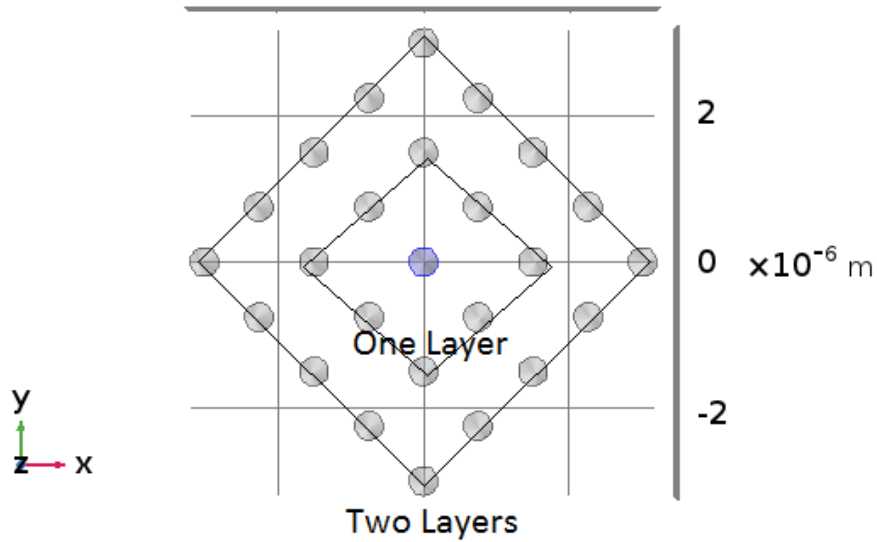
Figure 3.2: Top down view of two layers.

the fields produced at the tip of the central nanowire. After the fact, it became clear that only nanowires out to two layers have an influence on the central tip. As a result, we continue to work with a model that has 25 nanowires inside. This significantly increases the memory requirements necessary to run, but the study helped provide intuition on the system and circumvented the phantom solution issue.

3.3 Boundary Conditions

Neumann The side walls of the domain are filled with a zero charge boundary condition, which makes $n \cdot \vec{D} = 0$, where $\vec{D}$ is the displacement vector. This is appropriate since we are not interested in what happens outside of this boundary.

Dirichlet This sets the value of the field evaluated at the surfaces to a specific value. Here, the nanowires and bottom surface are set to $V = V_0 = 100V$, and the top plate is set to ground which is $V = 0$. Refer to Figure 3.3 for a visual.
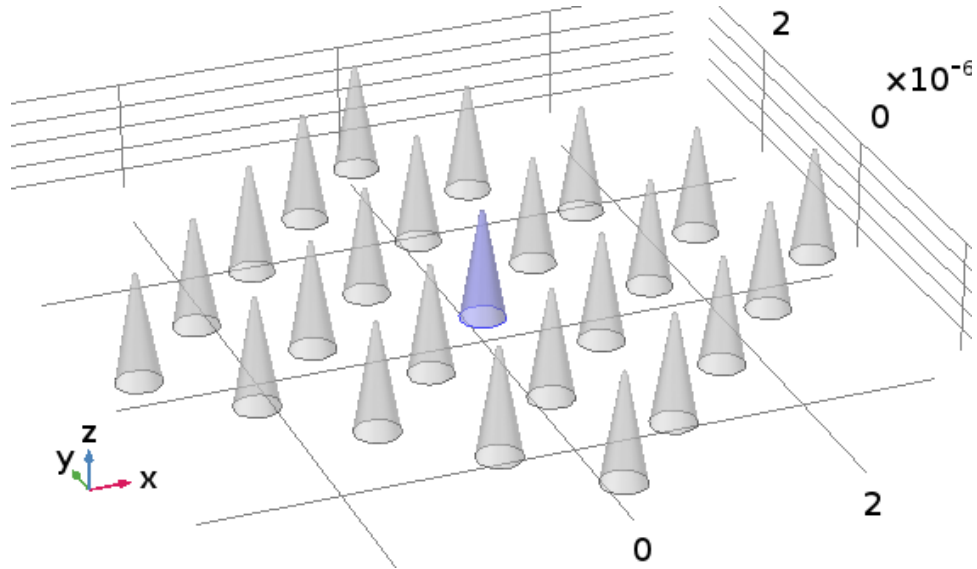
Figure 3.3: View of nanowire simulation domain.

3.4 Governing Equations

Laplace Equation Laplace's equation, a special case of Poisson's equation in free space, is the governing equation in this case since there are no charge distributions in this system (coupled with the previously discussed boundary conditions). Therefore our system looks like:

$$\nabla^2 V = 0$$

with boundary conditions ∂B defined in Section 3.3. In order to solve for the electric field distribution, COMSOL employs a finite element discretization to the Laplace equation, and uses a static solver to obtain a solution to the resulting linear system.

3.5 Particle Motion

In order to solve the DEP attraction problem I piped the force field obtained from the simulation into Newton's equations. To do this, I utilized the Mathematical Particle Tracing module in COMSOL. There are many options to doing this, such as Lagrangian or Hamiltonian formulations, but a straightforward Newtonian formulation works just fine. COMSOL solves $\frac{d(m_p \vec{v})}{dt} = \vec{F}$, given that the components

14
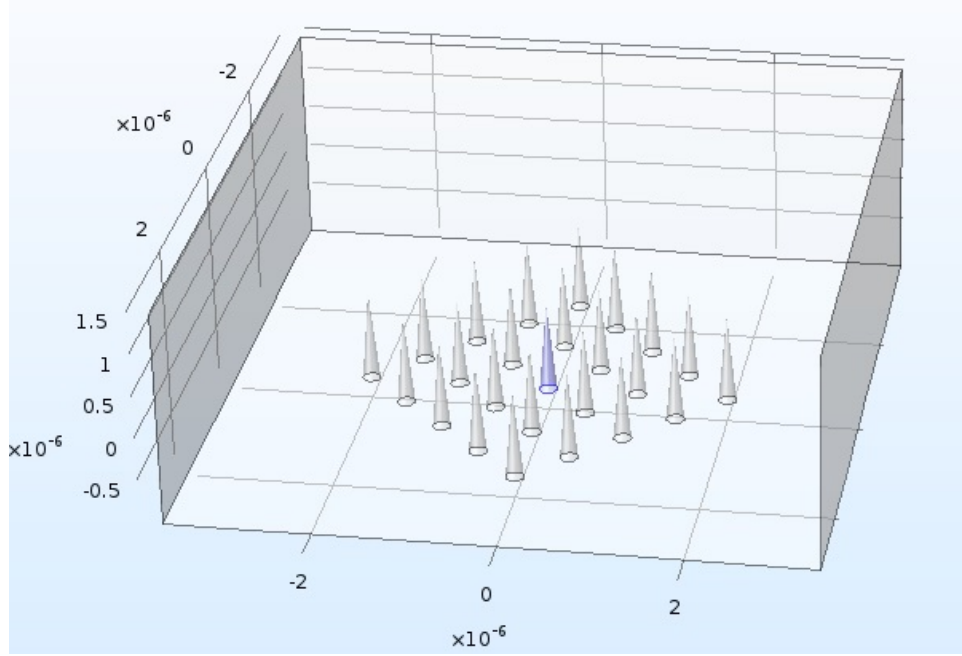
Figure 3.4: View of boundaries in the simulation. The nanowires and bottom face are biased to $V = V_0 = 100V$, the sides have zero charge boundary conditions, and the top face is biased.

of $\vec{F}$ are known.

Dielectrophoretic Attraction   Dielectrophoretic attraction is a term used to describe the interaction between a dipole moment and an electric field. This is interesting because even a neutral particle may interact with an electric field and alter its trajectory via this mechanism. A (perhaps strong) dipole moment may be induced given an affinity for polarization and an environment with sufficient electric fields. This force has the following form:

$$F_{DEP} = \frac{1}{2}\alpha\nabla|\vec{E}^2|$$ (3.3)

where α is the polarizability [14]. What this says is that there will be a force that points towards the direction of steepest change in the electric field. In this system, that will be towards the nanowire tips. I note here that in what follows we study

15

the effects of this force at various temperatures, and in actuality α is a function of temperature: $\alpha = \alpha(T)$. I'll argue that this is only important for certain elements in Chapter 5.

3.6   Gas Injection

Next we look at the properties of injecting gas into this system for particle tracing purposes. For this part we make the assumption that the gas is sparce, and therefore the particles are not interacting with each other. If this is the case, we do not need to solve the Navier-Stokes equations, and we can use the straightforward Newton's equations, significantly simplifying the problem.

Beam Geometry   An beam incident on the nanowire array will have a radius of $r_{beam} = 4r_0$. This was chosen so that the particles from the beam would sufficiently sample the space near the tips, and so that the deviations from the trajectories could be analyzed in earnest.

Gas Velocity   The final property that needs to be defined is the gas velocity, or the gas temperature. This will define in practice how much time a particle spends interacting with the strong fields near the tips. This simulation uses the RMS velocity, which is given by:

$$v_{rms} = \sqrt{\frac{3KT}{m}} \tag{3.4}$$

where m is the mass of the particle under question, and K is the Boltzmann constant.

Chapter 4

Numerical Results

4.1 Nanowire Study
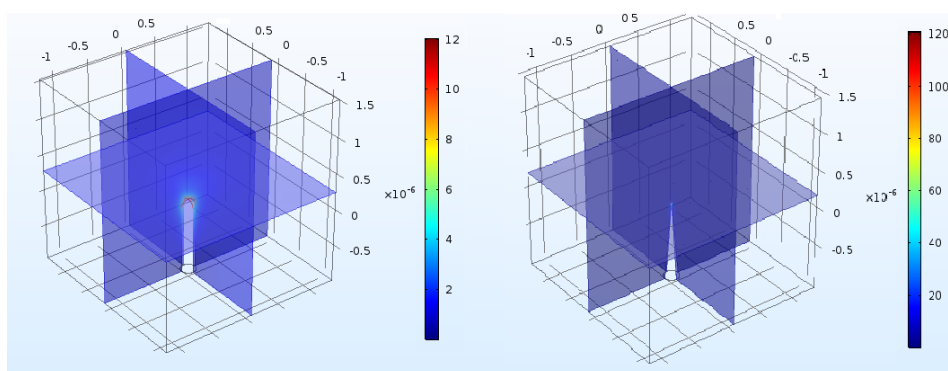
Figure 4.1: Results of sharpening. A 95nm vs 5nm radius of curvature.

Here we present the consequences of sharpening a nanowire, and apply the results to a field ionization experiment. I show that sharpening a nanowire of height 1um, base size 200nm, and radius of curvature equal to 100nm could reasonably multiply the field at the tip by over 100. Further, a nanowire array enclosed within a capacitor is studied, and the results of varying various system parameters are presented.

Next, I show that the nearest 24 neighboring wires are responsible for $\approx 95\%$ of the total shielding in a bulk array. This was concluded after a study showed that the difference in magnitude of shielding when taking into account 8 neighboring

nanowires vs 24 was only 5%.

Further, several well known properties of nanowire arrays were re-confirmed and extended for the case of sharpened wires. For example, there exists an ideal spacing between wires that balances shielding and fill density. It appears that an ideal pitch for a nanowire sharpened to 40nm shifts by about 1um compared to the unsharpened case.

Finally, a study of dielectrophoretic interactions on neutral particles near the tips is presented. Either the particle needs to have a large ratio between its polarizability and its mass, or the subsequent injected gas from which the particle comes from must be cooled. It is shown that when cooled to 3 K, two separate beams of Oxygen and Lithium both exhibit significant trajectory deviations *toward* the tips of the nanowires. This in principle means that the ionization cross section of a nanowire array indeed depends on the temperature of the gas injected, and *increases* when taken into account. As expected, Lithium (because of its favorable polarization to mass ratio) exhibits a much higher degree of attraction then Oxygen.

Array Shielding Effect On Field Enhancement As discussed earlier, the ideal simulation would use symmetry boundary conditions to simulate the rest of the array. However, this led to non-physical solutions. As a result, I took to simulating several layers of nanowires to see if I could still incorporate shielding effects. In order to perform this study, I ran several simulations with several geometries. In particular, three limiting cases of the bulk array are taken into account.

1. Three nanowires

2. One layer of nanowires

3. Two layers of nanowires.

Figure 4.2 shows the results of the study. Percent shielded is defined as

$$100 \cdot (1 - \frac{E_i}{E_{single}}) \qquad (4.1)$$

where i denotes the array approximation. As we can see, the addition of 16 nanowires to go from one layer to two layers (Figure 3.2) constitutes an approximate 5% increase in shielding. A resulting 3 layer simulation proved that the shielding change
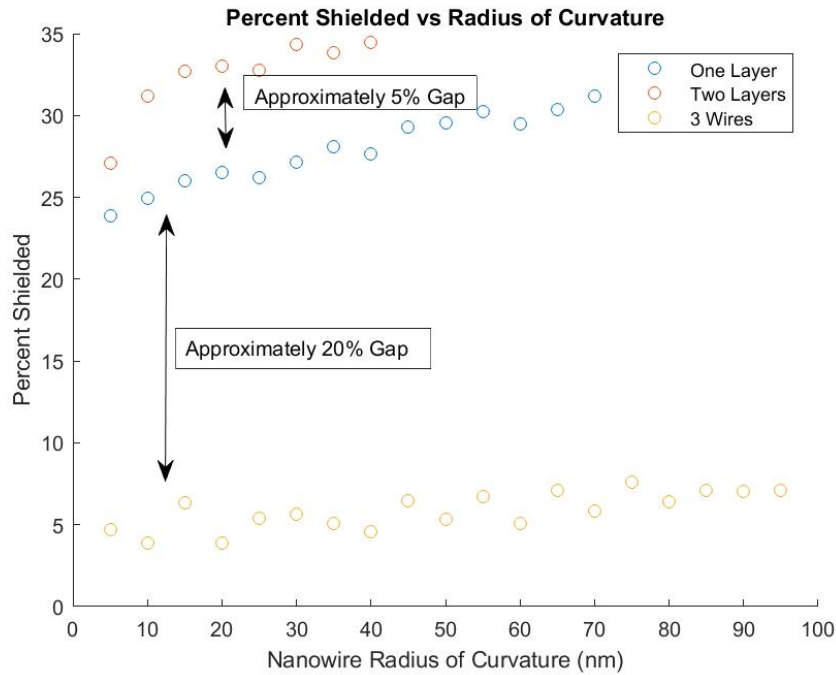
Figure 4.2: Percent Shielding for various geometries

from two layers to three layer geometry was insignificant directly, but the direct results are not shown here. This gives a heuristic that suggests a single nanowire effectively "sees" only two layers of wires surrounding it.

Pitch Effect On Field Enhancement The literature has numerous studies on electric fields at the tips of nanowires, however, the following question can be asked: "Does varying pitch and studying the electric field at the tip of a nanowire also depend on sharpness?" Figure 4.3 shows the results of this study. Indeed, the sharper the array, the larger $\frac{dE_{tip}}{d\delta}$ is. This intuitively makes sense, since the sharper tips provide less area for surface charge to distribute itself. It is also important to note that these graphs eventually asymptote to the single nanowire values as expected.

Capacitor Separation Effect On Field Enhancement In this section I present the results of studying how the separation of the capacitor plates effects the field at
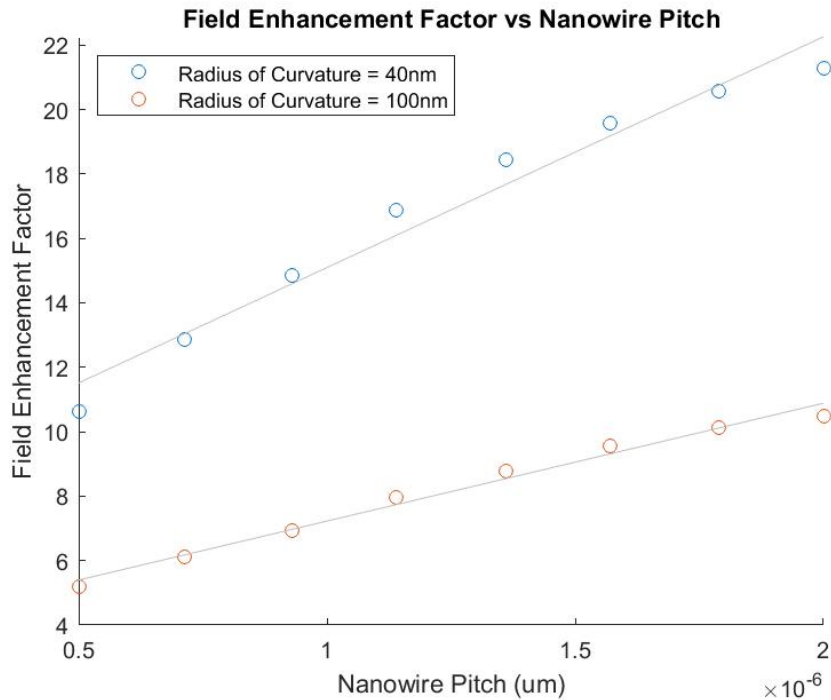
19

Figure 4.3: How Pitch Effects Nanowire Field Enhancement

the tip of the central nanowire. To naturalize units, all geometric properties of this system were defined in terms of H (the height of the nanowire). In this case, the plate separation can be thought of in terms of multiples of H. As we can see once the plate separation is approximately greater than $2H$, further separation has no effect on the nanowires. This has two useful corollaries:

- First, we have discovered a lower bound in the simulation domain for which further increase is a waste of computer memory (if capacitor effects are being ignored).

- And second, bringing the capacitor closer to the nanowires has a boosting effect to the field enhancement factor. This makes sense, since voltage gradients near the tips would intensify due to the field necessarily obeying boundary conditions.

The enhancement due to the plate separation is tiny, and will probably be difficult
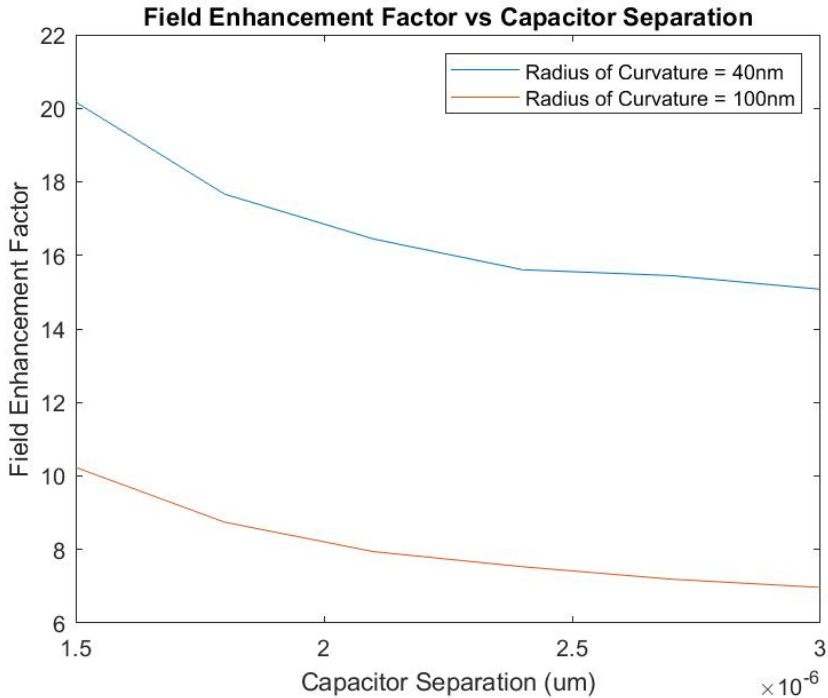
Figure 4.4: How Capacitor Size Effects Nanowire Field Enhancement

to implement experimentally due to electrostatic discharge, but was stated here for the sake of completeness.

Base varying Study   Here we present the results of the base varying study. It is interesting to note that all previous numerical simulations claimed that the FEF of a geometry only depends on its aspect ratio, as in Equation 2.2. Given the geometric analysis in Section 3.2, a tapered cone geometry is uniquely defined only after its base, radius of curvature, and height are defined. Indeed, we see that the FEF does depend on the base size, and is negatively correlated. As stated before, this makes sense because if the base is wider, there is a larger surface area for surface charges to distribute themselves, leading to a decrease in the charge density at the tip of the wire. However, what this study explicitly shows is that, even after increasing the base size approximately two-fold, the FEF only changes by 7.1% as seen in Table 4.1. This effectively explains why accurate numerical extrapolations can be made

ignoring base size: its functional dependence is weak.

Theta (Degrees)	FEF	Base (m)
2	15.87	3.89E-07
2.73	15.52	
3.45	15.53	
4.18	15.47	
4.91	15.28	
5.64	15.17	
6.36	15.05	
7.09	15.02	
7.82	15.07	
8.55	14.8	
9.27	14.59	
10	14.75	2.00E-07

Table 4.1: Parametric sweep of FEF's for various base sizes, holding $r_0 = 40nm$ and $H = 1um$ constant. Base size begins at 200nm, and progressively increases to 389nm.

Nanowire Sharpening Here we present the main results of this thesis, the gains to field enhancement factor due to nanowire sharpening. Figure 4.5 shows the results of sharpening a nanowire ($H = 1um$, $b = 200nm$, $r_0 = 100nm$). As the tip is sharpened, θ is solved for numerically to give the corresponding base size via Equation 3.1. Thus, sharpening leaving base size unchanged and provides a smooth geometry for the simulation to run on. Sharpening *significantly* increases the field enhancement factor of the nanowire tips.

As we can see, sharpening to 5nm provides an approximately 9x gain in the field enhancement factor. If the capacitor spacing is $d_{cap} = 2.5um$, then the bulk field is given by $E_{bulk} = \frac{bias}{d_{cap}}$. This evaluates to $4 \cdot 10^7 \frac{V}{m}$. This means that if we assume a FEF of about 100, which is reasonable according to the results, that means the field tips have a magnitude of order 10^9. Unfortunately, this means that nanowire sharpening alone will not achieve the orders of magnitude needed to ionize atoms such as Helium, which requires an electric field of about $2 \cdot 10^{10} \frac{V}{m}$ (Figure 4.6). However, sharpening the tips can get us within an order of magnitude.
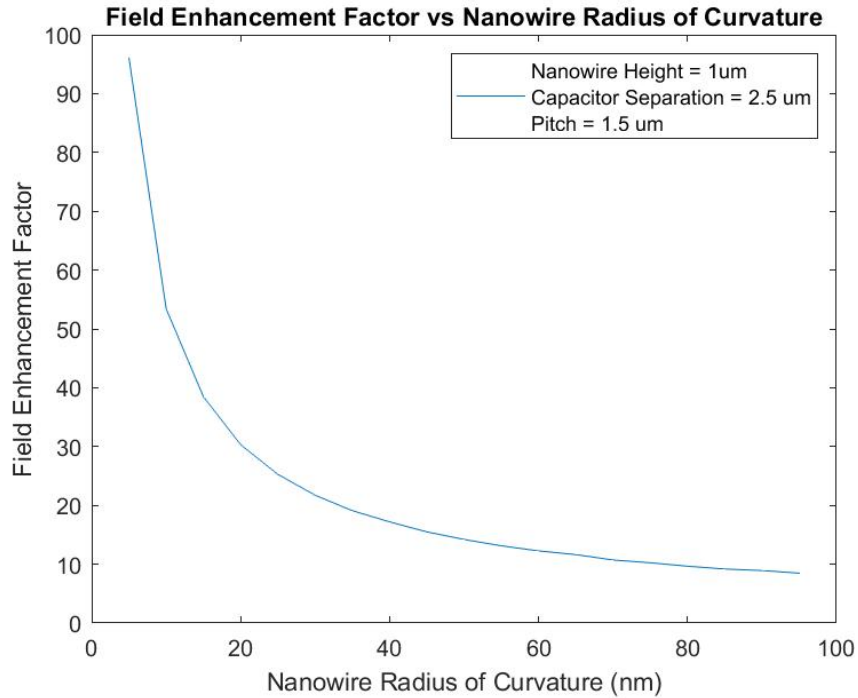
Figure 4.5: Field Enhancement Factor Gain From Sharpening

4.2 Dielectrophoretic Attraction Study

In this section I present the results of the particle trajectory study. Incorporating DEP coupling theoretically should pull neutral atoms towards the nanowire tips. If this effect is significant, then it would show that the ionization cross section of a sharpened nanowire array would in actuality be much higher then $2\rho r_0$, where ρ is the density of nanowires per unit area, r_0 is the radius of curvature of the wire. Two factors effect the amount of deflection that occurs due to the DEP force. From Newton's laws, we know that the smaller the mass of an object the larger the acceleration given an particular force. Since the DEP force does not depend on mass, it is a corollary that less massive particles are more susceptible to deviation. The second is the polarizability of the particle, since $F_{DEP} \propto \alpha$ (Equation 3.3). Given this information, a "DEP Relative Strength" can be defined as $\frac{\alpha}{m}$. From Table 4.2, we can expect that Lithium would exhibit the greatest trajectory deviations,

23
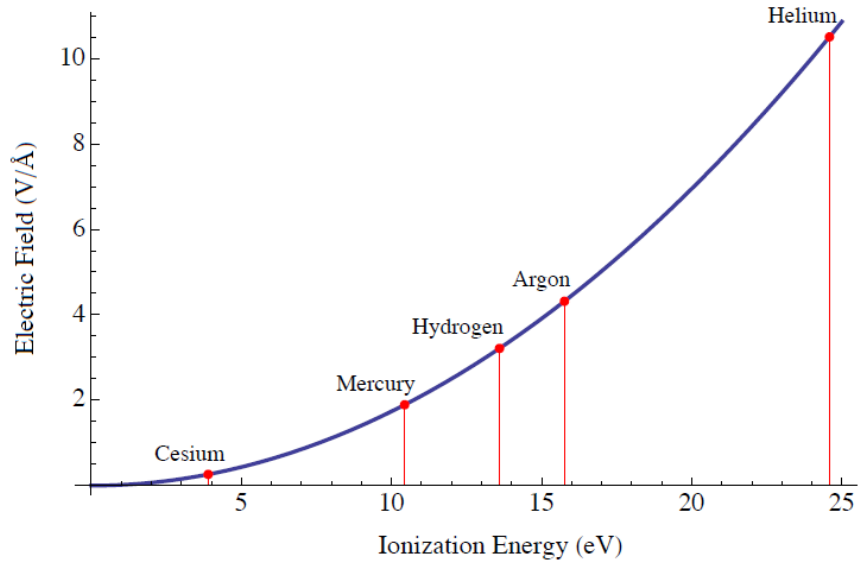
Figure 4.6: The electric field necessary to ionize various atoms in terms of binding energy for reference. Figure from [4]

.

whereas an element like Oxygen would be significantly less affected by the DEP interaction. Figure 4.7 and Figure 4.8 show that this is indeed the case. As we can see, in the case of Lithium, there is significant beam attraction even at room temperature. As we cool the gas further, particles are more and more attracted to the tips. In the case of Oxygen, we see that the DEP force only has a significant effect as $T \to 0$. This is because the v_{RMS} is sufficiently small at those temperatures that the DEP force has a longer time to interact with the constituents of the beam, and therefore has more effect in its deflection.
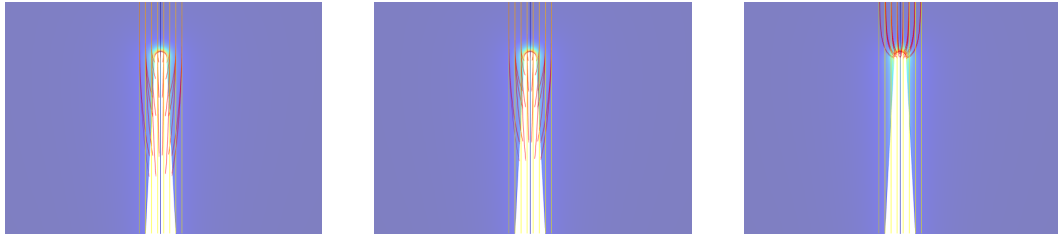
Figure 4.7: Lithium particle trajectories. From left to right: 293 K, 223 K, 3 K
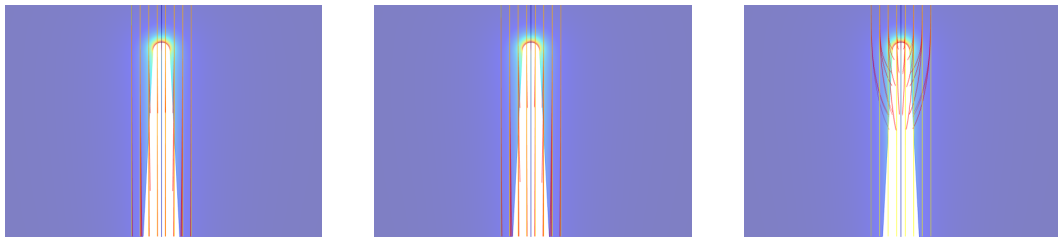
Figure 4.8: Oxygen particle trajectories. From left to right: 293 K, 223 K, 3 K

Element	Polarizibility (au)	Mass(amu)	DEP Strength	Ionization Energy (eV)
Ne	2.68	22.9897	0.12	21.564
F	3.76	20.1797	0.19	17.422
He	1.383	6.941	0.20	24.587
O	6.04	18.9984	0.32	13.618
N	7.43	15.9994	0.46	14.534
C	11	14.0067	0.79	11.26
H	4.5	4.0026	1.12	13.598
B	20.5	12.0107	1.71	8.298
Mg	71.7	24.305	2.95	7.646
Be	37.755	10.811	3.49	11.814
Na	162.6	24.305	6.69	5.139
Li	164	9.0122	18.20	5.392

Table 4.2: Ionization energies and DEP Relative Strength's for various elements, ordered in terms of increasing DEP Relative Strength.

Chapter 5

Discussion

5.1   Comments

In this thesis, I aimed to solve the problem of what would happen if a conical nanowire is sharpened. A-priori, it was unknown whether the thicker base would allow the surface charges to redistribute considerably. Given this issue, making the assumption that the base dimension is inconsequential would have been presumptuous. It turns out that the base dimension indeed has a slight effect on the FEF, and is one of the sources of the gap between truncated cone and conical wire geometry in Figure 2.2. However, the effect is relatively small. This suggests that there exists an extrapolation that has the same form as Equation 2.2 for the conical taper, though that was not studied here. However, numerical results are available in the literature for a conical tip grown on a tungsten ball [13], with an extrapolation of $2.1(\nu + .8)^{0.73}$. Differences between the simulation results presented in this thesis and in this paper would exemplify effects a spherical electrode would have to the field enhancement.

I'd like to make a quick comment about ignoring the temperature dependence of polarizability mentioned in Section 4.2. It was shown that for noble gasses, N_2, O_2, air, and CH_4, that the polarizability changes very little within the range $0K < T < 400K$ [15]. However, the polarizability of H_2 was shown to change by approximately 25% within the range $0K < T < 200K$. Even though the general trend is that the polarizability decreases as the temperature decreases, within room temperature to absolute zero, nearly all gas polarizabilities exhibited very weak to

negligible temperature dependences for this specific application. That being said, ignoring or neglecting the temperature dependence of the polarizability is therefore rigerously valid for some gasses. In the case that it isn't, the results presented in this thesis can be thought of as a best case scenario (since the polarizability is in fact larger than what it should be). In other words, for lack of necessity of a more in depth model, the particle deviation study demonstrated here can be safely assumed to be an *upper bound*.

For our specific field ionization setup, it appears that we are still about a factor of 10 away from achieving low voltage field ionization of gasses. However, there are papers that suggest augmenting geometric effects by gold doping the nanowires. Other nanowire enhancement modifications should be investigated to see if a factor of 10 can be achieved: this would push the FEF over the hump and allow for field ionization to be theoretically possible with this construction. Experiments attempting to do just that are being conducted by the Raizen Group at the time of writing this thesis.

5.2   Computational and Analytical Result Comparison

Field Enhancement Factor Comparison   Here I confirm that the results of the COMSOL simulation coincide with known results that were stated in the introduction. As we can see from both Figure 4.5 and Table 5.1, the FEF asymptotically approaches the correct value of $\gamma \approx \nu \approx 10$ as the sharpened geometry approaches that of a conical post. In addition, we see that the results are of the same order of magnitude across the board. The discrepancy between the flat electrode and spherical electrode simulations can be attributed to higher order effects due to the varied electrode geometry. We see that the magnitudes of the FEF's seem to be consistent with the results of the bound study as well [3].

r0 (nm)	Aspect Ratio	Numerical FEF	Cone On Sphere
95	10.53	12.64	12.35
90	11.11	12.94	12.81
85	11.76	13.68	13.32
80	12.50	14.14	13.89
75	13.33	15.04	14.52
70	14.29	15.57	15.23
65	15.38	16.71	16.03
60	16.67	17.39	16.94
55	18.18	18.83	18.01
50	20.00	20.17	19.25
45	22.22	21.92	20.73
40	25.00	23.77	22.53
35	28.57	26.55	24.76
30	33.33	29.82	27.63
25	40.00	34.25	31.48
20	50.00	41.24	36.94
15	66.67	52.03	45.44
10	100.00	71.17	60.92
5	200.00	126.24	100.75

Table 5.1: A comparison of relevant conical shape analyses. The numerical FEF here is for a *single* nanowire on a flat electrode.

Chapter 6

Conclusion

The work for this thesis began with a single question: would sharpening cylindrical post nanowires let the FEF at the tip reach magnitudes of $\approx 10^{10} \frac{V}{m}$? If so, low voltage field ionization would be a reality through geometric enhancements alone, and a variety of interesting applications could be realized.

6.1   Summary of Results

We began with looking at the simplest model of a protrusion, the semi-spherical bump on a plane. The exact electrostatic solution of this problem is well known, and yields a FEF of $\gamma = 3$. Next, we looked at the floating sphere on top of a plane model. This was introduced because the analytical approximation for the cylindrical wire follows very similar logic, and serves as a solid stepping stone. Then we get to the cylindrical wire case, and at this point we have a model that is widely used in the literature and has real world applications. Finally, we looked at a few numerical simulations and the more general hemi-ellipsoid solution.

Several older results in the literature such as electrode separation field enhancement and wire pitch shielding were reconfirmed and extended for the case of a conical-taper geometry. In addition, and to my knowledge novel, studies of FEF vs base size (Section 4.1), FEF through sharpening specifically (Section 4.1), and DEP coupling to neutral particles near the tips were presented (Section 4.2).

I showed that through geometric enhancements (under the constraint of operating at low voltages) fields reach magnitudes of approximately $10^9 \frac{V}{m}$, just an order

of magnitude off target. Though field ionization is not feasible exclusively through geometric enhancements, this thesis provides a platform to study other augmenting effects that could get fields past the ionization threshold.

The final question addressed in this thesis was whether DEP forces on neutral particles near the wire tips would significantly increase the ionization cross section. Performing a general analysis, the results shown in Table 4.2 show that DEP coupling has some attractive effect at room temperature for species with large $\frac{\alpha}{m}$. However, significant trajectory attraction towards the tip is only seen across the board once the gas beam has been cooled (Figure 4.7, Figure 4.8). This suggests that cooling a beam before injecting it into a nanowire setup could significantly increase the effectiveness of a nanowire field ionization device (if and when the order of magnitude discrepancy in field magnitude is addressed).

6.2   Concluding Remarks

A continuation of this work would likely include developing an extrapolation function, much like that produced for the other numerically simulated geometries. Improvements upon the model could obviously be made, however, the numerical results seem to be of sufficient stability and accuracy to be enough. To improve, one could attempt to correctly implement periodic boundary conditions as to simulate a true infinite array. This would have the added benefit of requiring less memory to store large field solutions (on the order of 2 GB per run), require less RAM for computation, and significantly reduce the rum-time (order of several minutes). In addition, a crude (free-tetrahedral mesh) was used for discretization. Since this system exhibits cylindrical symmetry, a more appropriate meshing strategy would be to use one that incorporates this symmetry. However, for our purposes the free-tetrahedral run was sufficient.

This system is simple (conceptually), exhibits a wide range of tweakable parameters to play with, and has flexibility in methods of construction. I'm very excited about the potential industrial application of these nanowires in medical sensing, field ionization, and photonics, and look forward to seeing where research progresses in this field in the near future.

Bibliography

[1] Takao Utsumi. Vacuum microelectronics: What's new and exciting. *IEEE Transactions on Electron Devices*, 38(10):2276–2283, 1991.

[2] Richard G Forbes, C J Edgcombe, and U Valdr. Some comments on models for field enhancement. Technical report.

[3] P. A. Chatterton. A theoretical study of field emission initiated vacuum breakdown. *Proceedings of the Physical Society*, 88(1):231–245, 1966.

[4] David Dunsky. Efficient Detection of Neutral Atoms via Electric Field Ionization. (May), 2016.

[5] Richard G Forbes. Refining the application of FowlerNordheim theory. *Ultramicroscopy*, 79(1-4):11–23, 9 1999.

[6] Wayne U Wang, Chuo Chen, Keng-Hui Lin, Ying Fang, and Charles M Lieber. Label-free detection of small-molecule-protein interactions by using nanowire nanosensors. 2005.

[7] Niels Gregersen, Torben R. Nielsen, Julien Claudon, Jean-Michel Gérard, and Jesper Mørk. Controlling the emission profile of a nanowire with a conical taper. *Optics Letters*, 33(15):1693, 2008.

[8] Kai Qiu, Yuhua Zuo, Tianwei Zhou, Zhi Liu, Jun Zheng, Chuanbo Li, and Buwen Cheng. Enhanced light trapping in periodically truncated cone silicon nanowire structure. *Journal of Semiconductors*, 36(10):2–7, 2015.

[9] Ashish Modi, Nikhil Koratkar, Eric Lass, Bingqing Wei, and Pulickel M. Ajayan. Miniaturized gas ionization sensors using carbon nanotubes. *Nature*, 424(6945):171–174, 2003.

[10] Medical uses of radioactive calcium. Technical report, IAEA.

[11] Yat Li, Jie Xiang, and Charles M Lieber. Nanowire electronic and optoelectronic devices. Technical report, 2006.

[12] Ramin Banan Sadeghian and M. Saif Islam. Ultralow-voltage field-ionization discharge on whiskered silicon nanowires for gas-sensing applications. *Nature Materials*, 10(2):135–140, 2011.

[13] C. J. Edgcombe and U. Valdrè. Microscopy and computational modelling to elucidate the enhancement factor for field electron emitters. *Journal of Microscopy*, 203(2):188–194, 2001.

[14] David J. Griffiths. *Introduction to Electrodynamics - Fourth Edition*. 2013.

[15] Klaus Keri, Uwe Hohm, and Hartmut Varcbrnin. Polarizability of Small Molecules. 1(I):728–733, 1992.